Advances in Nanomedicine and Nanotechnology Research
ANNR, 2(1): 77-88
www.scitcentral.com
ISSN: 2688-5476
Original Research Article: Open Access

Improvement in the Properties of α-Amylase Enzyme by Immobilization using Metal Oxide Nanocomposites as Carriers

Savitha DP, Bindu VU, Geetha G and Mohanan PV*

*Department of Applied Chemistry, Cochin University of Science and Technology, India.

Received August 13, 2019; Accepted August 27, 2019; Published June 25, 2020

ABSTRACT

Metal oxide Nano composites, ZnO-Fe_3O_4 (S1) and ZnO-PANI (S2) were synthesized and used as carriers for the immobilization of the enzyme, α-amylase. The parameters such as pH, temperature, concentration and contact time were optimized. The immobilized enzyme showed higher immobilization yield compared to that of the free enzyme. The thermodynamic parameters such as free energy change (ΔG°), entropy change (ΔS°) and enthalpy change (ΔH°) were evaluated and found to be higher for both S1and S2. The kinetic parameters, K_m and V_{max} were evaluated from Line weaver-Burk plots. The immobilized enzymes also showed higher storage stability and reusability which ensure them for various biochemical applications.

Keywords: ZnO-Fe_3O_4, ZnO-PANI, α-amylase, Immobilization, Catalytic activity, Thermal deactivation

INTRODUCTION

In the current global world, bio-catalysis is emerging as the most challenging field where there is increasing demand in applications with the highest biological impact. They also play a major role in the field of pharmaceutics, medical diagnostics [1,2], agrochemical products [3], cosmetics [4] and in food industry [5]. Bio-catalysis refers to the use of "enzymes" which reform them to process catalysts to execute under the reaction conditions of industrial process [6]. Interest in the field of immobilization of enzyme on solid supports and their applications have been emerging in the last few decades [7]. Immobilization intensifies the catalytic properties and makes them fit for many analyses [8].

Immobilization can be done by using various methods such as adsorption, covalent binding and entrapment within a porous matrix, microencapsulation and aggregation [9,10]. Adsorption is the simplest and widely used method for immobilization process which is based on physical adsorption or ionic binding [11,12]. The advantage of this method is that it minimizes the disturbance inactive centers thereby retains the entire amount of activity [13]. A wide variety of materials have been reported in literature which is used as carriers for immobilization process [14-17]. Presence of more reactive sites with good mechanical properties makes nanocomposite materials more notable to possess several applications. Nanocomposites formed by combination of conducting polymers and metal oxides nanoparticles, possess the good properties of both the constituents and thus enhance the utility [18]. Zinc oxide structured metal oxides are more advantageous over other nano metal oxides, makes it a favorable material for enzyme immobilization [19]. Since, magnetite particles allow easy separation of the catalyst from the reaction and with high surface area are more used in immobilization of enzymes in an effective way [20,21]. Magnetite particles also have the capability to improve the efficiency of the immobilized enzymes by weakening the diffusion barriers in transporting the substrate and the reaction products [22]. Polyaniline (PANI), one of the most versatile and environmentally stable polymers having high stability to extreme pH and temperature makes suitable for enzyme immobilization [23,24].

The enzyme α-amylase was chosen as the enzyme for immobilization. It is one of the enzymes with great significance in miscellaneous fields [25,26]. They are endo enzymes that cleave α-1,4 glycosidic bonds in poly-

Corresponding author: PV Mohanan, Department of Applied Chemistry, Cochin University of Science and Technology, India, E-mail: mohan@cusat.ac.in

Citation: Savitha DP, Bindu VU, Geetha G & Mohanan PV. (2020) Improvement in the Properties of α-Amylase Enzyme by Immobilization using Metal Oxide Nanocomposites as Carriers. Adv Nanomed Nanotechnol Res, 2(1): 77-88.

saccharides which results in the production of glucose, maltose and maltotriose units [27]. The survey of literature reveals that a wide variety of work had been done in the immobilization of α-amylase [28-33].

In our study, we immobilized α-amylase onto magnetite-ZnO (S1) and PANI-ZnO (S2) nanocomposites. The method used is adsorption. The nanocomposites were characterized by IR, TGA, XRD and SEM analysis. Effect of different immobilization parameters such as pH, temperature, contact time and amount of enzyme required for immobilization were evaluated to achieve maximum immobilization yield and efficiency. The kinetic parameters K_m and V_{max} were calculated from the Lineweaver-Burk plots. The thermal deactivation studies were performed and thermodynamic parameters were evaluated. Thermal stability, reusability and storage stability of the enzyme were studied under free and immobilized conditions.

MATERIALS AND METHODS

Materials

Diastase α-amylase (1,4 α-D-gluconglucanohydrolse, E. C. 3.2.1.1) was purchased from HiMedia Laboratories Pvt. Ltd, Mumbai. Soluble Starch (potato) and aniline were procured from S. D. Fine Chem. Ltd. Mumbai. Iron (II) chloride. Tetrahydrate ($FeCl_2.2H_2O$), Zinc acetate dehydrate ($Zn(CH_3COO)_2$, Hydrochloric acid (HCl), Ammonia solution (NH_3, 25%), Ammonium peroxodisulphate and acetone were purchased from Merck Co.

Synthesis of ZnO-Fe_3O_4 nanocomposite (S1)

ZnO-Fe_3O_4 nanocomposite was prepared on the basis of already reported work [34]. Initially, magnetite nanoparticles were prepared by dissolving 1 g of $FeCl_2.4H_2O$ 100ml of distilled water. 15 ml of NH_3 solution (5 M) was added slowly with continuous stirring. The acquired precipitate was black. It was then centrifuged, cleansed several times with distilled water further dried and weighed. About 1 g of the magnetite nanoparticles were dissolved in distilled water and Zn $(CH_3COO)_2.2H_2O$ was added and dissolved in the same solution. 5ml of ammonia (5 M) was slowly added to the above solution. The precipitate obtained was then filtered, rinsed with distilled water and dried at 200°C.

Synthesis of ZnO-PANI nano composites (S2)

ZnO nanoparticles were first prepared by adding NaOH containing 2 M ethanol was added drop wise to the ethanolic solution of zinc nitrate drop by drop for about 2 h. The solution is allowed to stand overnight. The precipitate settled may contain unwanted contents which is removed by rinsing with distilled water for three times and also with ethanol and dried at around 60°C [35]. ZnO-PANI nanocomposite was prepared by dissolving 1 g of ZnO powder in 20 mL aqueous solution of 0.01 mol aniline and 0.01 mol hydrochloric acid. 0.01 mol of APS was made to dissolve in 100 ml distilled water, further was added drop wise to the above mixture with stirring in an ice bath for 5.5 h. The precipitate was obtained which is again filtered, washed with distilled water and ethanol and dried at 500°C [36].

Characterization of synthesised nanocomposites

The synthesized nanocomposites were characterized by FT-IR spectrometry using JASCO FT/IR-4100. Bruker AXS D8 Advance is used for XRD analysis. SEM images were obtained by using the JEOL Model JSM-6390LV scanning electron microscope. Thermal behavior of the nanocomposites was obtained by using Perkin Elmer, Diamond TG/DTA.

Immobilization of enzyme, α-amylase

Immobilization of enzyme was carried out by mixing the synthesized nanocomposites with equal volumes of enzyme in buffer solution followed by shaking in a water bath shaker at room temperature for two hours. The prepared biocatalyst was rinsed with the same buffer to remove the unbound enzyme. The unbound enzyme in the supernatant and washings were estimated by the spectrophotometric method, using Folin-Ciocaltaue's phenol reagent by measuring the absorption at 660 nm in Thermo scientific evolution 201 UV-Visible Double Beam Spectrophotometer. The freshly prepared immobilized enzyme was stored in a refrigerator at 4°C for further studies [37].

Immobilization yield (IY) was calculated by measuring concentration of protein in supernatants before and after immobilization, according to Eqn 1,

$$IY\% = \frac{C_1 - C_2}{C_1} X\ 100 \qquad (1)$$

Where C_1 was the concentration of protein taken for immobilization and C_2 was the concentration of protein present in supernatant after immobilization. And the activity yield (AY) was determined by the Eqn 2,

$$AY\% = \frac{\text{Activity of immoblized enzyme}}{\text{Activity of free enzyme}} X\ 100 \qquad (2)$$

The immobilization efficiency (IE) was calculated using Eqn 3,

$$IE = \frac{AY}{IY}(\%) \qquad (3)$$

Activity determination of the free and immobilized enzyme

The activity of immobilized α- amylase was observed using starch as the substrate. The reagent used was 3,5-dinitrosalicylic acid (DNS). The test tubes containing the reaction mixture (1 ml each of α-amylase and 1% starch) with desired buffer are shaken thoroughly for 15 min at room temperature. 3,5-dinitrosalicylic acid (1 ml) was then added to each of the test tubes to stop the reaction. Incubation was done in a boiling water bath for 5 min and

cooled until room temperature is attained. The amount of sugar (maltose) produced was determined spectrophotometrically at 540 nm [38].

Conditions for optimization of free and immobilized enzymes

The optimization of the immobilization parameters such as pH, temperature, concentration and contact time was done. The maximum activity of optimum pH was assayed using starch in enzyme and incubated over a pH range 4-9 at 30°C. The optimum temperature for maximum activity was performed by varying the range of temperature from 30°C to 70°C. Thermal stabilities for free and immobilized enzyme were investigated by measuring their residual activities at optimum conditions after being incubated for 60 min in the temperature range of 30-60°C in a water bath and then cooled to optimum temperature. Desired amount of 1% starch was added to each reaction at definite time interval to carry out the reaction process.

Kinetic studies of free and immobilized enzymes

Free and the immobilized enzymes was incubated at different temperatures without adding starch to perform the kinetic studies. The enzyme activity assay was done at definite time intervals and the residual activity is expressed in terms of percent of initial activity. The deactivation constant (kd) is obtained from the slope of the logarithmic plot of percent residual activity versus time and the slope of Arrhenius plot drawn between ln kd and reciprocal of temperature, 1/T (K) gives the deactivation energy (Ed) using Eqn 4,

$$\text{Slope} = -\frac{\text{Ed}}{R} \quad (4)$$

Thermodynamic parameters

Estimation of the values of thermodynamic parameters such as free energy change (ΔG°), entropy change (ΔS°), and enthalpy change (ΔH°) can be obtained using kd and Ed values.

$$\Delta H^\circ = Ed - RT \quad (5)$$

$$\Delta G^\circ = -RT \ln \frac{kd.h}{k_B.T} \quad (6)$$

$$\Delta S^\circ = \frac{\Delta H^\circ - \Delta G^\circ}{T} \quad (7)$$

Where R is the universal gas constant, T is the absolute temperature (K), h is the Planck constant and k_B is the Boltzman constant.

Determination of kinetic parameters

Michaelis constant (K_m) and maximum rate (V_{max}) are the kinetic parameters that can be evaluated from Lineweaver-Burk plot. Initial reaction rate were measured under optimum conditions of pH and temperature by changing the concentration of starch.

Reusability and storage stability

The reusability study of the immobilized enzyme was done using batch experiment by maintaining the fixed hours for each cycle. The residual activity of the immobilized enzyme at optimum pH and temperature was measured at fixed time intervals. At the end of each cycle, the immobilized enzyme was removed and washed with buffer and then added a substrate solution to begin a new cycle. The process is done for several counts. The stability while storing immobilized enzyme in buffer solution for a long time was measured by calculating their activities after being stored at 4°C for several months. At regular intervals of time, assay was performed. The activity obtained was compared with the initial one and considers as the percentage relative activity.

RESULTS AND DISCUSSION

Characterization studies of the synthesized nanocomposites

The FT-IR spectrum of ZnO exhibits broad absorption peaks between 3500 and 3600 cm^{-1}, corresponding to the stretching mode of O–H group of hydroxyl group and the weak band near 1630 cm^{-1} is assigned to H–O–H bending vibration mode due to the adsorption of moisture on the surface of nanoparticles. The band 3477 cm^{-1} corresponds to the stretching vibrations of the OH group on the surface of ZnO nanoparticles. The peaks observed in the region 460-390 cm^{-1} corresponds to the Zn-O bond. The spectrum of Fe_3O_4, the peak in the region 3600-3100 cm^{-1} is attributed to the stretching vibrations of –OH, which is assigned to –OH (water molecules) absorbed by Fe_3O_4 nanoparticles, the peak in the region 570-590 cm^{-1} is attributed to the Fe-O bond vibration of Fe_3O_4. The spectrum of S1 **(Supplementary Data – Appendix A)** shows Fe–O bond around 565 $cm^{-1.}$ In order to confirm existence of Zn–O bond in nanocomposite, ZnO nanoparticles were prepared in absence of Fe_3O_4 by the same method and its FT-IR spectrum is shown. It can be observed that the strong absorption band at 435 cm^{-1} which is ascribed to phonon absorptions of the ZnO lattice is present. The spectrum exhibits broad absorption peaks between 3500 and 3600 cm^{-1}, corresponding to the stretching mode of O–H group of hydroxyl group and the weak band near 1630 cm^{-1} is assigned to H–O–H bending vibration mode due to the adsorption of moisture on the surface of nanoparticles. The PANI show characteristic peaks at 503.1cm^{-1}, 587.6cm^{-1}, 798.7cm^{-1}, 1121.8cm^{-1}, 1296.7cm^{-1}, 1472.4cm^{-1}, 1559.8cm^{-1}, 2369.3cm^{-1} and 3446.7cm^{-1} corresponds to C=N iminoquinone, C=C stretching modes of quinoid rings, the C=C stretching mode of benzenoid rings, the stretching mode C-N, C-H bending mode of aromatic rings. The S2 composite **(Supplementary data – Appendix A)** also show the same characteristic peaks. But some of the peaks of PANI were shifted to higher values which may be due to the hydrogen bonding between ZnO and NH_2 group of PANI on the surface of ZnO particles.

The XRD peaks of S1 and S2 are shown in **Appendix B**. The strong and sharp peaks of S1 are found at 2θ=35.6°, 43.1°, 53.5°, 62.7°, corresponding to (311), (400), (422) and (440) crystal planes of face centered cubic Fe_3O_4 respectively (JCPDS file no: 75-0033). FCC structure of Fe_3O_4 retained even after the formation of nanocomposite. The XRD peaks of ZnO are found at 2θ=31.7°, 34.36°, 36.2°, 56.59°, 62.7° and 67.90° corresponding to (100), (002), (101), (110), (103) and (112) planes assigned to the wurtzite pattern of ZnO (JCPDS card 36-1451). The characteristic peak of polyaniline were at 2θ=26°. Using Debye Scherrer equation, the average particle size can be evaluated quantitatively.

$$d = k\lambda / \beta\cos\theta$$

Where, d gives the particle size, k is the Debye Scherrer constant (0.89), λ is the X- ray wavelength (0.15406 nm), β is the full width at half maximum and θ is the Bragg angle. According to this equation, the particle size of S1 is 24.5 nm and of S2 is 21.8 nm.

The surface morphology was observed from the SEM analysis. The SEM micrographs of S1 show that the magnetite nanoparticles are well dispersed on ZnO and are found to be loosely packed. The SEM image of S2 reveals that ZnO particles are surrounded by polyaniline matrix and appears as aggregated particle structure **(Appendix C)**.

The TG-DTG curve of the S1 and S2 are shown in **Appendix D**. All of them underwent two stages of weight loss. The first stage of weight loss from room temperature to 200°C is ascribed to loss of water molecules. The reason behind the weight loss between 250°C and 550°C may be due to the decomposition of the polymer chain which occurs before 490°C in pure samples. The interaction with ZnO nanoparticles reduces the decomposition and makes S1and S2 more thermally stable compared to pure samples [39].

Conditions optimized for immobilization

To find out the optimum immobilization conditions for the enzyme, we have inquired the effect of pH of the immobilization medium, effect of temperature of the immobilization medium, contact time of carrier and amount of enzyme taken for immobilization. The activity which is retained during optimization was represented in terms of relative activity. **Figure 1a** shows the effect of pH on immobilization process. The optimum pH for both S1 and S2 was obtained at pH 6. At pH 6, there is an effective surface interaction between the carriers and the enzyme there by showing the highest activity. Because of the lack of considerable interaction, there is a decrease in the activity at higher pH.

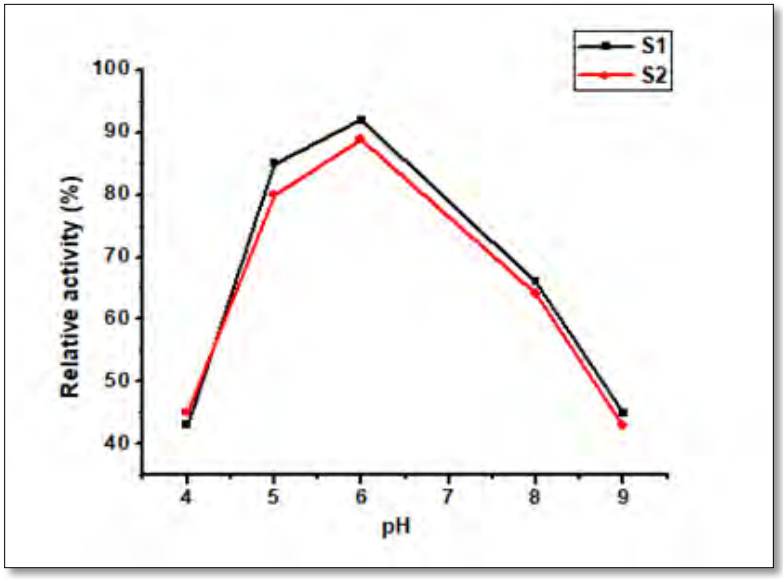

Figure 1a. Effect of pH on immobilization of α-amylase.

By keeping other parameters constant, the adsorption time was varied from 30-150 min. **Figure 1b** shows the effect of contact time after immobilization. The relative activity of enzyme is high for S1 at 60 min and that of S2 is at 120 min. The contact time is more for S2 compared to that of S1. Enzyme activity first increased with increase in contact time, longer an enzyme is incubated with the carriers, greater the amount of product will be formed. As a result, the rate of formation of product slows down as the incubation proceeds. After that even if the contact time of enzyme increased, the activity was found to be decreased which might be due to lower accessibility of substrate as a result of multilayer adsorption of enzyme and also be due to the formation of a disordered multilayer or formation of multiple bonds which deformed the active site of the enzyme [40].

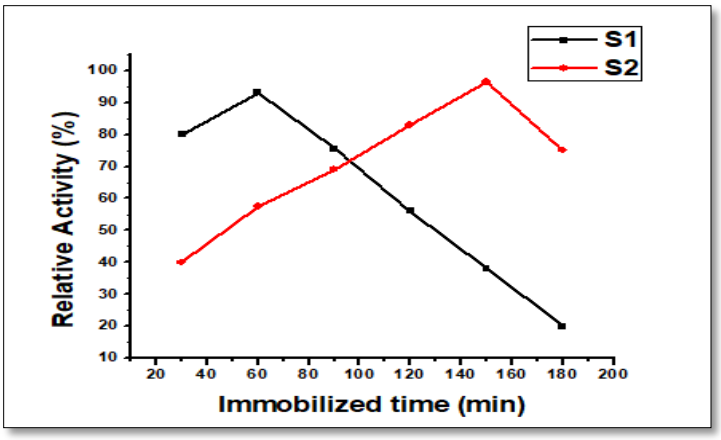

Figure 1b. Effect of contact time on immobilized enzyme activity.

Figure 1c shows the effect of enzyme loaded at optimum pH 6. The protein loaded and the enzyme activity **(Figure 1d)** increases as the concentration increases and reaches the maximum and then decreases which shows the formation of monolayer. After the saturation point the enzyme starts to desorb from the surface of the support. The amount of adsorbed protein depends on the strength of interaction between enzyme and the support and the method of immobilization [41]. The immobilization yield, activity yield and immobilization efficiency were calculated and the results are given in the **Table 1**.

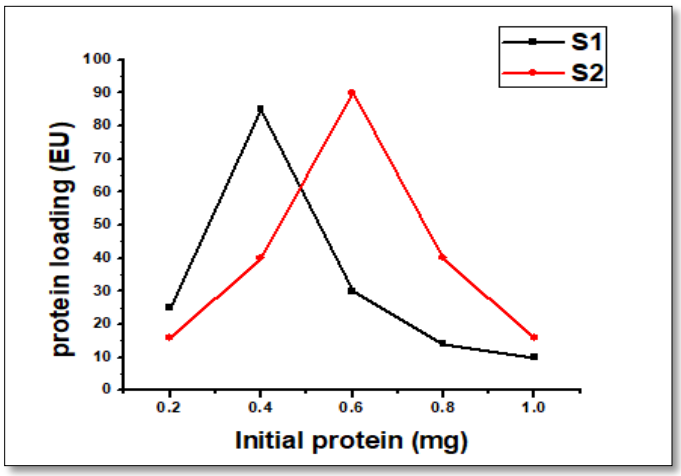

Figure 1c. Effect of initial protein amount on protein loading.

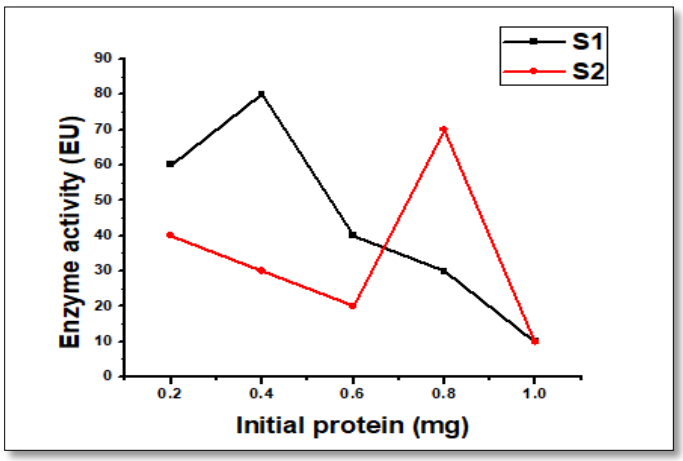

Figure 1d. Effect of initial protein concentration on immobilized enzyme activity.

Table 1. Immobilization efficiencies of S1 and S2.

Support	Initial protein (mg/ml)	Immobilized protein (mg/ml)	Immobilization yield (%)	Activity yield (%)	IE=AY/IY (%)
S1	0.4	0.38	85	80	94.1
S2	0.6	0.41	90	70	77.7

Parameters affecting the activity of enzymes

Effect of pH on the enzyme activity: We have examined the effect of pH on free and immobilized enzymes at a range of pH 4-9 and the results shown in **Figure 2a**. The maximum activity of free enzyme was found to be at pH 5.5. After immobilization, the optimum pH has been changed to pH 7. These results also prove that the process of immobilization shields the enzyme from alkaline and severe acidic medium [42]. After immobilization, the stability has increased which may be due to low diffusional limitations.

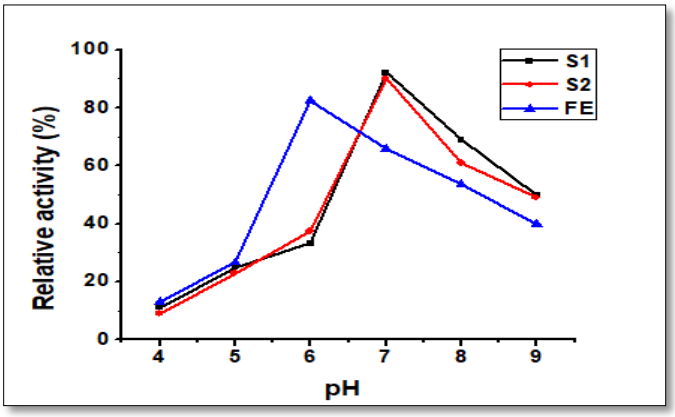

Figure 2a. Effect of pH on the activity of free and immobilized enzyme.

Effect of temperature on the enzyme activity: The effect of temperature on the activity of free and immobilized enzymes (S1 and S2) was investigated at a temperature range from 30°C to 70°C and shown in **Figure 2b**. The optimum temperature for starch hydrolysis was found at 50°C for free enzyme. The immobilized enzymes S1 showed maximum activity at 50°C and S2 at 45°C. The decrease in optimum temperature might be due to the change in conformational integrity of the enzyme structure by immobilization which favored amylase activity below 50°C. The higher temperature may lead to the denaturation of enzyme. The lowering of optimum temperature was reported when polyaniline used for the immobilization of glucoamylase [43].

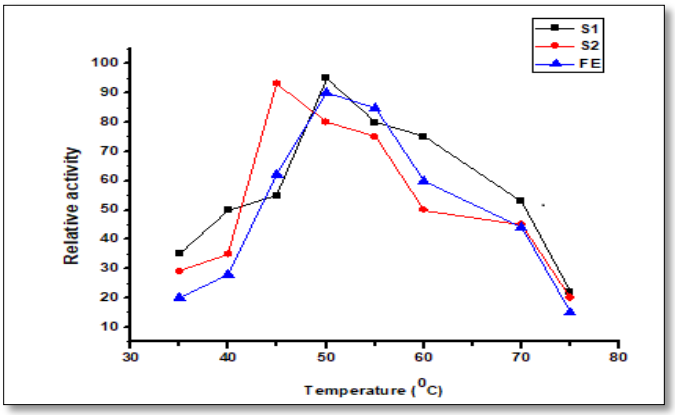

Figure 2b. Effect of temperature on the activity of free and immobilized enzyme.

In order to estimate the activation energy, Ea, an Arrhenius plot was drawn between log relative activity (%) and 1/T (K) **(Figure 2c)**. Values obtained were 16.99, 24.02 and 27.07 for free enzyme, S1 and S2, respectively. The activation energy was found to be decreased which might be due to the

loss of conformational integrity at the enzyme active site after immobilization.

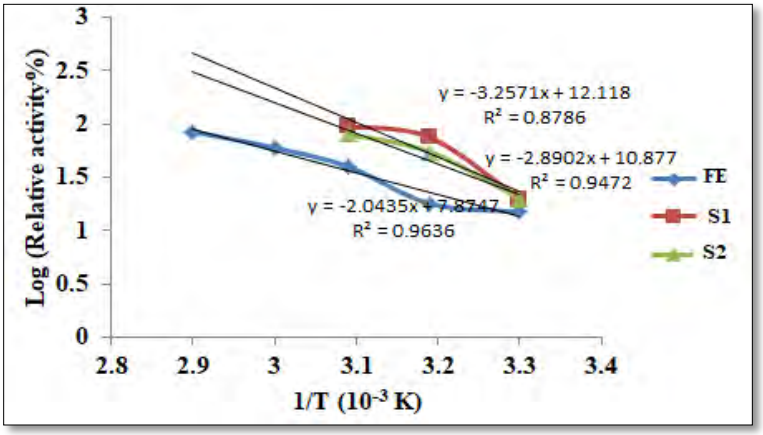

Figure 2c. Arrhenius plot of free and immobilized enzyme.

Thermal stability

Enzymes which are susceptible to industrial applications should be thermally stable. In order to investigate this property of the free and immobilized enzymes, it was incubated in buffer in solution for 60 min in a water bath over the temperature range of 30-70°C. The results **(Figure 3)** obtained reveals the high heat resistance of S1 and S2 compared to free enzyme. Both free and immobilized enzymes show high-rise in activity after 60 min of pre incubation at 30°C. The stability was found to be decreased as the temperature rises. When the temperature reached at 70°C, free enzyme lost almost 90% of the activity whereas S1 and S2 lost 30-35%. With reference to adsorption, increase in thermal stability was attributed to increase in enzyme rigidity due to strong electrostatic interaction of carriers with free enzyme which retains the tertiary structure of enzyme from conformational changes that might occur at higher temperatures [44].

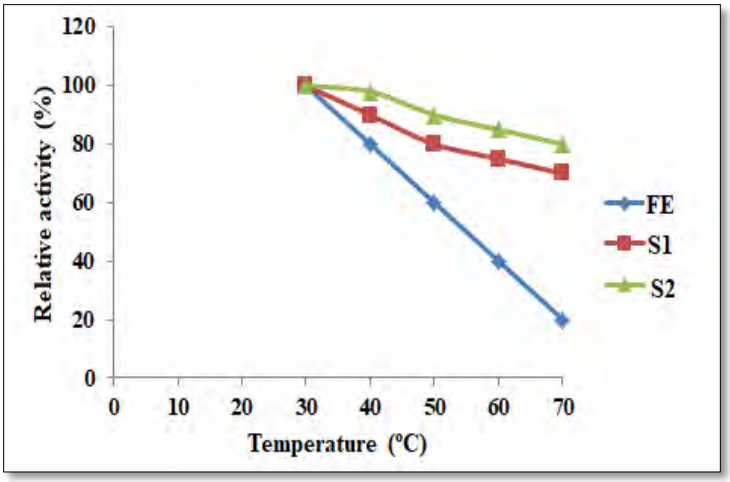

Figure 3 Thermal stability of free enzyme, S1 and S2.

Thermal inactivation and kinetics

The thermal inactivation study of free and immobilized enzymes were conducted by pre incubation at various incubation times at their respective optimum temperature and the corresponding relative activity was determined. The log relative activity (%) versus time plot illustrates the first law of thermodynamics [45]. The plot of ln kd and 1/T **(Figure 4)** whose slope of the linear curve gives the deactivation energy (Ed) of both free and immobilized enzymes. The values for Ed were 18.9, 21.6 and 27.4 for free enzyme, S1 and S2, respectively. After immobilization, the Ed values were found to be enhanced which makes them more stable towards denaturation and also reveals the requirement of higher energy for thermal deactivation and makes them more potent towards industrial applications [46,47].

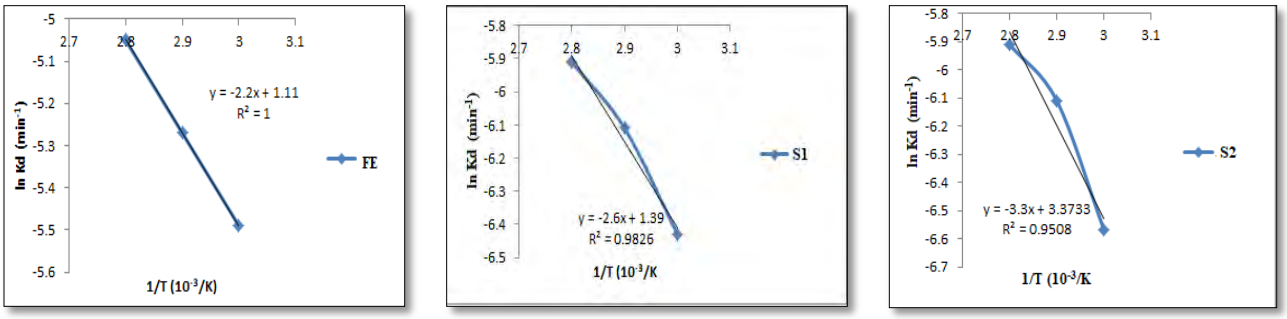

Figure 4. Arrehenius plot to calculate deactivation energy.

Evaluation of thermodynamic parameters

The feasibility and spontaneous nature of the biosorption process was reflected by the thermodynamic parameters [48]. The enthalpy change (ΔH°) at 60°C, for free enzyme was 15.52 KJ mol^{-1}, S1 was 18.83 KJ mol^{-1} and for S2, 24.63 KJ mol^{-1} **(Table 2)**. The enhancement in temperature decreases the value of ΔH° in all cases indicated that lower amount of energy is needed for the denaturation of enzyme at high temperatures. As a result of immobilization, greater amount of energy is required for the thermal denaturation of enzymes at high ΔH° values [49]. The higher Gibbs free energy change (ΔG°) of the immobilized enzymes describes that at high temperature, the thermal unfolding is controlled by the immobilization process and also increase in thermal stability provides resistance towards the thermal denaturation [50]. The ΔG° values at 60°C, for free enzyme, S1 and S2 were 108.27 KJ mol^{-1}, 110.87 KJ mol^{-1} and 111.21 KJ mol^{-1}, respectively and are tabulated in **Table 2**. The negative values of entropy of deactivation (ΔS°) showed the processes of ordered state which enhances the stability of enzyme through strong intermolecular forces [51]. Taking the magnitude values, S1 and S2 have lower values compared to free enzyme that indicated their ordered state which were enhanced due to immobilization.

Table 2. Thermodynamic parameters of free and immobilized enzymes at different temperatures.

Temperature	Enzyme	ΔG° KJ mol^{-1}	ΔH° KJ mol^{-1}	ΔS° KJ mol^{-1}
60°C	FE	108.27	15.52	-0.2785
	S1	110.87	18.83	-0.2764
	S2	111.21	24.63	-0.2600
70°C	FE	110.87	15.44	-0.2782
	S1	113.36	18.75	-0.2758
	S2	113.34	24.54	-0.2589
80°C	FE	113.55	15.36	-0.2781
	S1	116.51	18.67	-0.2771
	S2	116.85	24.46	-0.2617

Kinetic parameters

The two most important parameters to characterize the kinetic properties of the enzyme are K_m, the Michelis constant and V_{max}, the maximum reaction velocity from Michelis-Menton kinetics. K_m and V_{max} for free enzyme, S1 and S2 were evaluated from Line weaver Burk plots **(Figure 5)**. These parameters were studied by varying the concentration of starch in the reaction medium. K_m gives the measure of affinity of enzyme active site for its substrate. High K_m values specify lower substrate affinity for the enzyme [52]. K_m value for the free enzyme is lower compared to S1 and S2 **(Table 3)**. V_{max} is the maximum catalytic potential of the enzyme. There was a reduction in the value of V_{max} which might be due to immobilization. It changes the conformations of enzyme which leads to decrease in affinity to the substrate [53,54].

Table 3. Kinetic constants K_m and V_{max} of free and immobilized enzymes from Lineweaver Burk plots.

Catalyst	Free enzyme	S1	S2
K_m (mg/ml)	0.61	0.65	0.83
V_{max} (mg/ml/min)	18.69	18.2	18.4

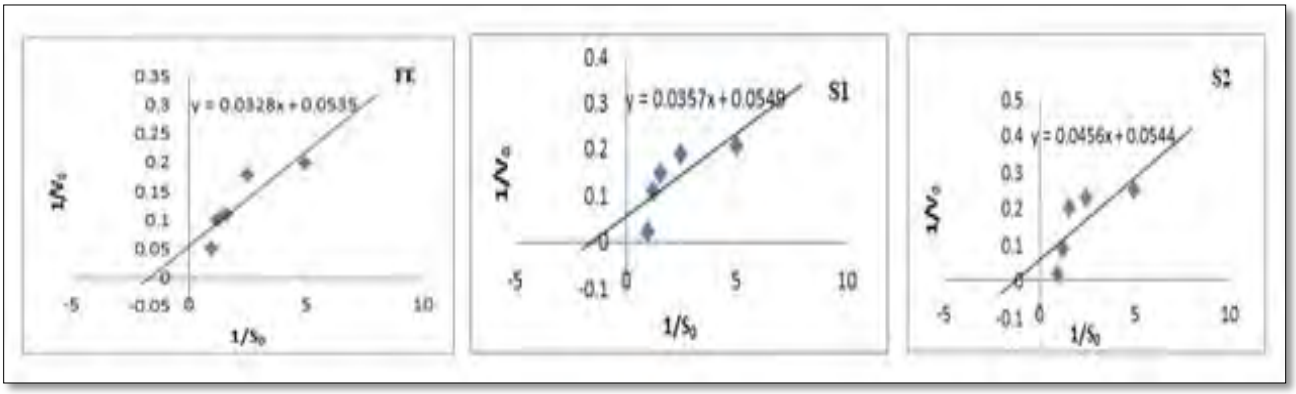

Figure 5. Lineweaver Burk plots of free enzyme, S1 and S2.

Reusability

The major advantage of the immobilized process is the repeated use of enzymes which makes them cost effective for industrial applications. Reusability of the enzymes was evaluated in a repeated batch process. S1 retained 55% and S2 to 54% activity after 5 cycles **(Figure 6)**. In the 8th cycle, the activity of S1 and S2 reached to 20% and cannot be reused further. The decline in activity might be due to denaturation and desorption of the enzyme molecules. Reusability studies of α-amylase have been outlined in literature [55,56].

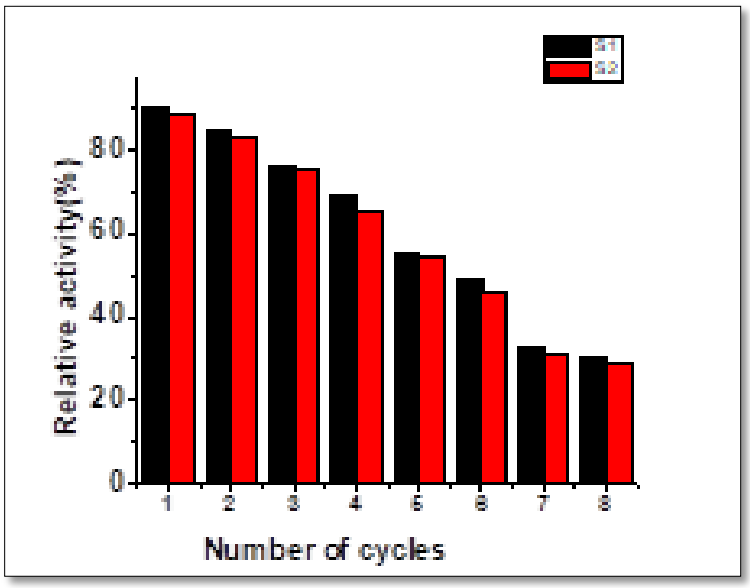

Figure 6. Reusability of the immobilized enzyme S1 and S2.

Storage stability

Efficiency in storage of an enzyme is an important criterion for the applications in industry. The immobilized enzymes cannot maintain their stability and activity for long term storage in its dried form. So, it was then stored in buffer solution at 4°C to exhibit high activity and stability. Immobilized enzyme S1 retained 76% and S2 retained 72% after 2 weeks. After 6 weeks, S1 reduced to 50% and S2 to 45%. The results **(Figure 7)** suggested that the immobilized enzyme exhibit improved storage stability. This decrease in activity among the immobilized enzymes is due to the time-dependent natural loss in activity of enzymes.

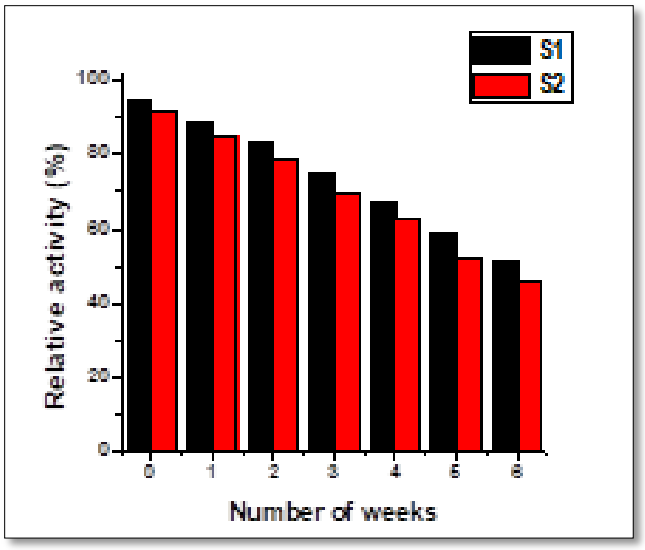

Figure 7. Storage stability of the immobilized enzyme S1 and S2.

CONCLUSION

ZnO-Fe_3O_4 (S1) and ZnO-PANI (S2) composites were successfully prepared. The composites were confirmed by FT-IR, XRD, TGA and SEM images. The α-amylase was successfully immobilized onto S1 and S2 nanocomposites. The parameters of immobilization were optimized. Immobilization brought about an increase in the Km value but a decline in the V_{max} and the changes correspond to immobilization induced conformational changes in the enzyme. The immobilized enzymes S1 and S2, shows good thermal stability, reusability and storage stability compared to the free enzyme. Thermodynamic parameters ΔH°, ΔG°, ΔS° were determined whose values indicated that due to immobilization the stability increased at high temperatures. These results suggest that both S1 and S2 was a good support for immobilization of α-amylase and suitable for various industrial applications.

ACKNOWLEDGEMENT

The author is thankful to UGC for financial support.

REFERENCES

1. Xiang CC, Chen Y (2000) cDNA microarray technology and its applications. Biotechnol Adv 18: 35-46.
2. D'Orazio P (2003) Biosensors in clinical chemistry. Clinica Chimica Acta 334: 41-69.
3. Benkovic SJ, Ballesteros A (1997) Biocatalysts - The next generation. TIBTECH 15: 385-386.
4. Wegman MA, Janssen MHA, Rantwijk FV, Sheldon RA (2001) Towards biocatalytic synthesis of β-lactam antibiotics. Adv Synthesis Catalysis 343: 559-576.
5. Gavrilescu M, Chisti Y (2005) Biotechnology - A sustainable alternative for chemical industry. Biotechnol Adv 23: 471-499.
6. Illanes A (2008) Enzyme biocatalysis: Principle and application. Springer: New York, p: 391.
7. Veesar IA, Solangi IB, Memon S (2015) Immobilization of α-amylase onto a calix [4] arene derivative: Evaluation of its enzymatic activity, Bioorg Chem 60: 58-63.
8. Guisan JM (2006) Methods in biotechnology. Immobilization of Enzymes and Cells, 2nd Edn.
9. Altinkaynak C, Tavlasoglu S, Özdemir N, Ocsoy I (2016) A new generation approach in enzyme immobilization: Organic-inorganic hybrid nanoflowers with enhanced catalytic activity and stability. Enzyme Microb Technol 93-94: 105-112.
10. Messing RA (1976) Adsorption and inorganic bridge formations. In: Methods in Enzymology (Mosbach K, ed.), Academic Press, New York, XLIV 44: 148-169.
11. Woodward J (1985) Immobilized enzymes: Adsorption and covalent coupling. In: Immobilized Cells and Enzymes: A Practical Approach (Woodward J, ed.), IRL, Oxford, UK, pp: 3-17.
12. Bindu VU, Mohanan PV (2017) Enhanced stability of α-amylase via immobilization onto chitosan-TiO_2 nanocomposite. Nanosci Technol 4: 1-9.
13. Wu L, Wu S, Xu Z, Qiu Y, Li S, et al. (2016) Modified nanoporous titanium dioxide as a novel carrier for enzyme immobilization. Biosensors Bioelectronics 80: 59-66.

14. Miao F, Lu X, Tao B, Li R, Chu PK (2016) Glucose oxidase immobilization platform based on ZnO nanowires supported by silicon nanowires for glucose biosensing. Microelectron Eng 149: 153-158.

15. Guncheva M, Dimitrov M, Zhiryakova D (2011) Nanosized tin dioxide - Unexplored carrier for lipase immobilization. Catalysis Commun 16: 205-209.

16. Lee D-G, Ponvel KM, Kim M, Hwang S, Ahn IS, et al. (2009) Immobilization of lipase on hydrophobic nano-sized magnetite particles. J Mol Catalysis B Enzymatic 57: 62-66.

17. Yakimova R, Selegard L, Khranovskyy V, Pearce R, Spetz AL, et al. (2012) ZnO materials and surface tailoring for biosensing. Front Biosci 4: 254-278.

18. Ali SMU, Ibupoto ZH, Salman S, Nur O, Willander M, et al. (2011) Selective determination of urea using urease immobilized on ZnO nanowires. Sensors Actuators B Chem 160: 637-643.

19. Srivastava N, Singh J, Ramteke PW, Mishra P, Srivastava M (2015) Improved production of reducing sugars from rice straw using crude cellulase activated with Fe_3O_4/alginate nanocomposite. Bioresour Technol 183: 262-266.

20. Yang L, Guo Y, Zhan W, Wang Y, Lu G (2014) One-pot synthesis of aldehyde-functionalized mesoporous silica-Fe_3O_4 nanocomposites for immobilization of penicillin G acylase. Microporous Mesoporous Mater 197: 1-7.

21. Yucebilgic G, Gulesci N, Yildirim D (2016) Immobilization and characterization of urease onto different spacer arms attached magnetic nanoparticles. New Biotechnol 104: 33.

22. Stejskal J, Kratochvil P, Jenkins AD (1996) The formation of polyaniline and the nature of its structures. Polymer 37: 367-369.

23. Gospodinova N, Terlemezyan L (1998) Conducting polymers prepared by oxidative polymerization: Polyaniline. Progr Polym Sci 23: 1443-1484.

24. Pandya PH, Jarsa RV, Newalkar BL, Bhalt PN (2005) Studies on the activity and stability of immobilized α-amylase in ordered mesoporous silica. Microporous Mesoporous Mater 77: 67-77.

25. Alva S, Anupama J, Savla J, Chiu YY, Vyshali P, et al. (2007) Production and characterization of fungal amylase enzyme isolated from *Aspergillus* sp. JGl12 in solid state culture. Afr J Biotechnol 6: 576-581.

26. Kalburcu T, Tuzmen MN, Akgol S, Denizli A (2014) Immobilized metal ion affinity nanospheres for alpha-amylase immobilization. Turk J Chem 38: 28-40.

27. Kiran KK, Chandra TS (2008) Production of surfactant and detergent-stable, halophilic and alkali tolerant α-amylase by a moderately halophilic *Bacillus* sp. strain TSCVKK. Appl Microbiol Biotechnol 77: 1023-1031.

28. Tripathi P, Kumari A, Rath P, Kayastha AM (2007) Immobilization of α-amylase from mung beans (*Vigna radiata*) on A mberlite MB 150 and chitosan beads: A comparative study. J Mol Catalysis B Enzymatic 49: 69-74.

29. Kahraman MV, Bayramoğlu G, Kayaman-Apohan N, Güngör A (2007) α-amylase immobilization on functionalized glass beads by covalent attachment. Food Chem 104: 1385-1392.

30. Bellino MG, Regazzoni AE, Soler-Illia GJ (2010) Amylase-functionalized mesoporous silica thin films as robust biocatalyst platforms. ACS Appl Mater Interfaces 2: 360-365.

31. Jaiswal N, Prakash O, Talat M, Hasan SH, Pandey RK (2012) α-amylase immobilization on gelatin: Optimization of process variables. J Genet Eng Biotechnol 10: 161-167.

32. Kumar RSS, Vishwanath KS, Singh SA, Rao AGA (2006) Entrapment of α-amylase in alginate beads: Single step protocol for purification and thermal stabilization. Process Biochem 41: 2282-2288.

33. Pascoal AM, Mitidieri S, Fernandes KF (2011) Immobilisation of α-amylase from *Aspergillus niger* onto polyaniline. Food Bioprod Process 89: 300-306.

34. Jilla S, Noshin M, Davood G, Khandan-Barani K, Alireza H, et al. (2015) Sonochemical synthesis of Fe_3O_4/ZnO magnetic nanocomposites and their application in photo-catalytic degradation of various organic dyes. J Mater Sci Mater Electron 26: 9591-9599.

35. Talam S, Karumuri SR, Gunnam N (2012) Synthesis, characterization and spectroscopic properties of ZnO nanoparticles. ISRN Nanotechnol 2012: 6.

36. Deepa J, Shanthi RJ (2016) Synthesis, characterization and fluorescence applications of conducting poly o-phenylenediamine and its ZnO nanocomposites. Int J Sci Res Methodol 5: 522-535.

37. Lowry OH, Rosebrough NJ, Farr AL, Randall RJ (1951) Protein measurement with the Folin phenol reagent. J Biol Chem 193: 265-275.

38. Jaiswal N, Prakash O, Talat M, Hasan SH, Pandey RK (2012) α-amylase immobilization on gelatin: Optimization of process variables. J Genet Eng Biotechnol 10: 161-167.

39. Daikh S, Zeggai FZ, Bellil A, Benyoucef A (2018) Chemical polymerization, characterization and

electrochemical studies of PANI/ZnO doped with hydrochloric acid and/or zinc chloride: Differences between the synthesized nanocomposites. J Phys Chem Solids 121: 78-84.

40. Bindu VU, Shanty AA, Mohanan PV (2018) Parameters affecting the improvement of properties and stabilities of immobilized α-amylase on chitosan-metal oxide composites. Int J Biochem Biophys 6: 44-57.
41. Ashly PC, Joseph JM, Mohanan PV (2011) Activity of diastase α-amylase immobilized on polyanilines (PANIs). Food Chem 127: 1808-1813.
42. Esawy MA, Mahmoud DAR, Fattah AFA (2008) Immobilization of *Bacillus subtilis* NRC33a levansucrase and some studies on its properties. Braz J Chem Eng 25: 237-246.
43. Silva RN, Asquieri ER, Fernandes KF (2005) Immobilization of *Aspergillus niger* glucoamylase onto a polyaniline polymer. Process Biochem 40: 1155-1159.
44. Zhao G, Wang J, Li Y, Huang H, Chen X (2012) Reversible immobilization of glucoamylase onto metal-ligand functionalized magnetic FeSBA-15. Biochem Eng J 68: 159-166.
45. Pal A, Khanum F (2011) Covalent immobilization of xylanase on glutaraldehyde activated alginate beads using response surface methodology: Characterization of immobilized enzyme. Process Biochem 46: 1315-1322.
46. Driss D, Driss Z, Chaari F, Semia EC (2014) Immobilization of His-tagged recombinant xylanase from *Penicillium occitanis* on nickel-chelate eupergit C for increasing digestibility of poultry feed. Bioengineered 5: 274-279.
47. Kishore V, Gowda SKR, Swati K, Kusha S, Rashmi M, et al. (2014) Bovine serum albumin a potential thermostabilizer: A study on α-amylase. J Appl Environ Microbiol 2: 37-41.
48. Baysal Z, Bulut Y, Yavuz M, Aytekin C (2013) Immobilization of a-amylase via adsorption onto bentonite/chitosan composite: Determination of equilibrium kinetics and thermodynamic parameters. Starch/Stärke 66: 484-490.
49. Bhatti H, Zia A, Rakhshanda N, Sheikh MA, Muhammad HR, et al. (2005) Effect of copper ions on thermal stability of glucoamylase from *Fusarium* sp. Int J Agric Biol 7: 585-587.
50. Pal A, Khanum F (2010) Characterizing and improving the thermostability of purified xylanase from *Aspergillus niger* DFR-5 grown on solid-state-medium. J Biochem Technol 2: 203-209.
51. Anema SG, McKenna AB (1996) Reaction kinetics of thermal denaturation of whey proteins in heated reconstituted whole milk. J Agric Food Chem 44: 422-428.
52. Kalantari M, Kazemeini M, Tabandeh F, Arpanaei A (2012) Lipase immobilisation on magnetic silica nanocomposite particles: Effects of the silica structure on properties of the immobilised enzyme. J Mater Chem 22: 8385-8393.
53. Hosseinipour SL, Khiabani MS, Hamishehkar H, Salehi R (2015) Enhanced stability and catalytic activity of immobilized a-amylase on modified Fe_3O_4 nanoparticles for potential application in food industries. J Nanoparticle Res 17: 382.
54. Chang MY, Juang RS (2005) Activities, stabilities and reaction kinetics of three free and chitosan-clay composite immobilized enzymes. Enzyme Microb Technol 36: 75-82.
55. Swarnalatha V, Esther RA, Dhamodharan R (2013) Immobilization of α-amylase on gum acacia stabilized magnetite nanoparticles, an easily recoverable and reusable support. J Mol Catalysis B Enzymatic 96: 6-13.
56. Hasirci N, Aksoy S, Tumturk H (2006) Activation of poly (dimer acid-coalkyl polyamine) particles for covalent immobilization of α-amylase. Reactive and Functional Polymers 66: 1546-1551.